Brain Pathology 9: 219-235(1999)

RESEARCH ARTICLE

Response of Glia, Mast Cells and the Blood Brain Barrier, in Transgenic Mice Expressing Interleukin-3 in Astrocytes, an Experimental Model for CNS Demyelination

Henry C. Powell [1], Robert S. Garrett [2], Francesca M. Brett [2], Chi-Shuin Chiang [3], Emily Chen [3], Eliezer Masliah [2] and Iain L. Campbell [3]

[1] Veterans Administration Research Service, VAMC San Diego
[2] Department of Pathology, University of California San Diego
[3] Department of Neuropharmacology, The Scripps Research Institute, La Jolla, CA 92037.

Transgenic mice overexpressing cytokines facilitate analysis of the effects of these immunomodulators on indigenous cells of the central nervous system. This study examines morphological aspects of demyelination and permeability changes, in a recently described transgenic model (termed GFAP-IL3). GFAP-IL3 mice develop progressive motor disease at approximately 5 months. Lesions identified after disease onset, showed activation of microglia, astroglial proliferation with phagocytosis of lipids, and immigration of macrophages and mast cells into neural parenchyma. Lymphocytes failed to appear until the later stages of the disease. Later, cerebellar and brain stem white matter contained focal demyelinating lesions with intense macrophage infiltration and a proliferative astrocytosis. Dystrophic axonal changes were noted, in addition to demyelination in heavily infiltrated lesions. Mast cells, variably present in the thalamus and meninges of wild type mice, were greatly increased at these sites in GFAP-IL3 mice. Blood-brain barrier (BBB) defects were documented with leakage of intravenously injected horseradish peroxidase. Mast cell infiltration into the CNS and their degranulation at the site of injury, may represent initial events in a spontaneous process of macrophage mediated demyelination in which glial cells and macrophages are both involved in the phagocytic process.

Corresponding author:
Henry C. Powell MD., DSc., MRCPath, Department of Pathology, 9500 Gilman Drive, La Jolla, California 92093-0612.
Tel.: + 619 534 3717; Fax: + 619 534 0391;
E-mail; hpowell@ucsd.edu

Introduction

Resident central nervous system cells such as astrocytes, endothelia and microglial cells are known to respond to cytokines and in concert with inflammatory cells, play a role in developing and sustaining the disease process involved in inflammatory demyelination (31). Transgenic murine models for cytokine overexpression provide new means to evaluate the impact of these immunomodulators in neurodegenerative and demyelinating disease (8, 9, 48, 52, 53) and it is becoming increasingly clear that there are distinctive neuropathologic changes associated with activity of specific transgene encoded cytokines (8, 9, 10, 12, 48, 52, 53). Here we have used one of these models to investigate the response of indigenous CNS cells to inflammatory demyelination. The GFAP-IL3 mouse is a recently described model of macrophage/microglial activation in which affected mice develop normally before displaying symptoms of motor incapacity at approximately 5 months of age, followed by steady deterioration and death at 6-8 months of age (12). Immunolocalization, molecular and initial neuropathologic studies reveal that this disease involves inflammation associated with focal demyelination, advancing to cavitary destruction of white matter which was present at the time of death, in animals with the most severe neurologic abnormalities. The mechanism of demyelination is unique, in that although it is mediated by inflammatory cells, T and B cells do not appear to be involved in the initial process (12). There is activation of perivascular microglial cells and infiltration of brain parenchyma by circulating mononuclear cells as well as mast cells, which appear on the brain surface and within lesions within the brains of affected animals. The appearance of focal lesions suggests a local alteration in vascular permeability in affected regions of the brain. This calls for further study of the response of astrocytes and endothelial cells which play a key role in maintaining the selective permeability of the blood brain barrier. In this paper we show that the onset of inflammatory demyelination in the GFAP-

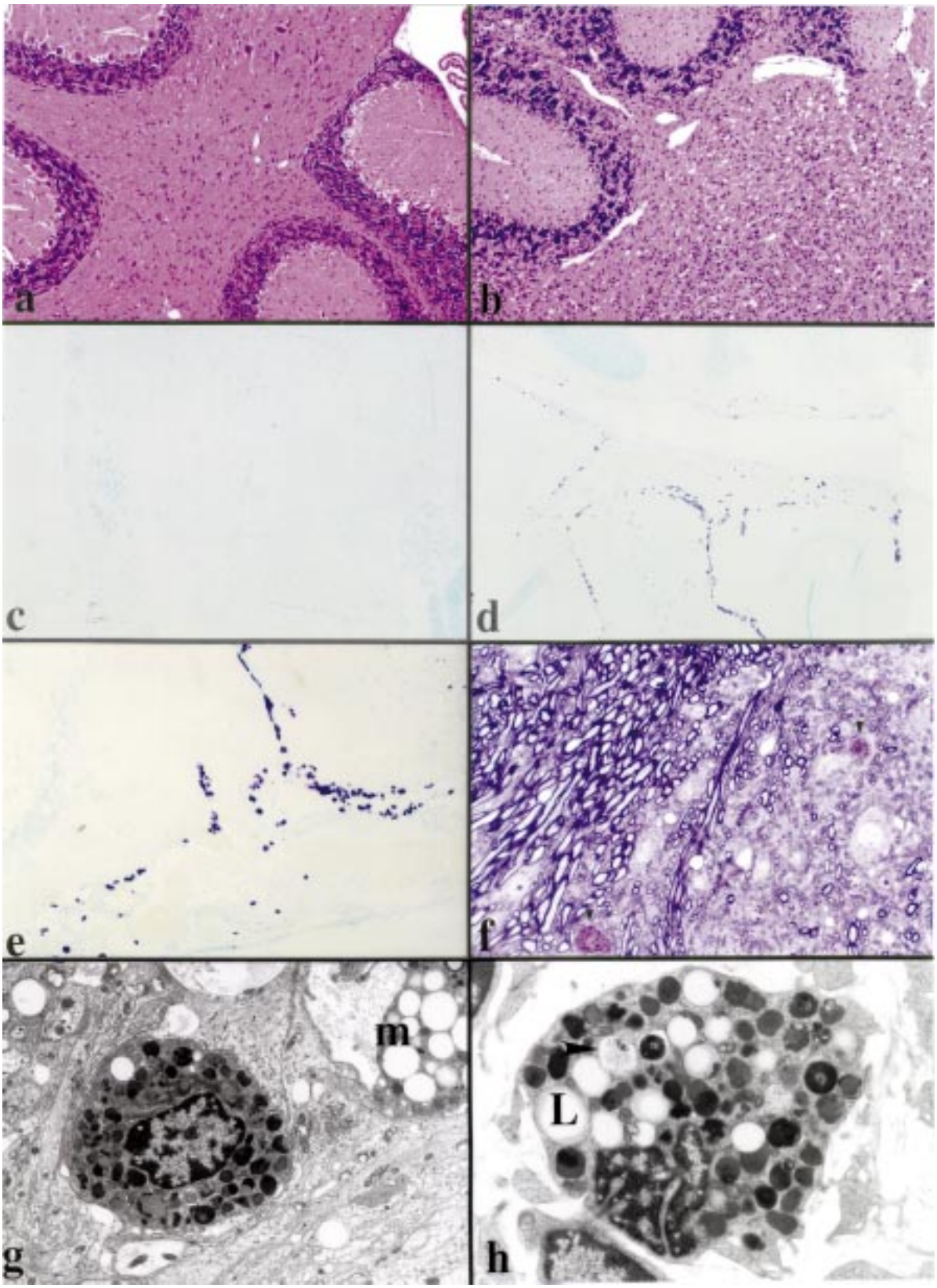
a
b
c
d
e
f
m
g
L
h

IL3 mouse, coincides with increased mast cell activity and altered vascular permeability. In addition, demyelination is macrophage mediated, with oligodendrocyte survival and activation of astrocytes which play a part in the phagocytosis of lipid debris generated by myelin breakdown. While the role of macrophage/microglia in the pathogenesis of the inflammatory demyelinating disease in the GFAP-IL3 mice is well established (12), the response of resident cells known to be involved in human MS (31) requires further morphologic analysis. Thus we have examined in more detail in this transgenic model, the role of the mast cell, the astrocyte, and the BBB, in relation to the macrophage/microglia and the demyelinating lesion as well as the impact of the inflammatory infiltrate on axons within this lesion.

Methods

Transgenic mice. The development of the GFAP-IL3 transgenic mice has been already reported (12) and transgenic mice from the G3C2 line were used in this study. GFAP-IL3 mice were identified by slot-blot analysis of tail DNA using a ^{32}P-labeled SV-40 late region DNA fragment as a probe. Offspring from this transgenic line remain healthy until approximately 5 months of age before developing the motor disorder described previously (12). Asymptomatic animals aged four months (n=5), symptomatic animals aged from 4 (n=2) to 6 (n=18) months and age-matched non-transgenic litter mate controls (n=6) were used in this study. Symptomatic mice were sacrificed when physical signs of motor impairment were first apparent, in order to facilitate comparison of cytopathologic abnormalities.

Histology. Tissue was prepared for both light and electron microscopy (EM) with paraffin and plastic embedding. Immunolocalization studies were performed either on frozen sections or paraffin embedded tissue, or on resin embedded tissue for electron microscopy. Prior to perfusion with a fixative solution, animals were deeply anesthetized by an intraperitoneal injection (2ml/mg) of a solution consisting of pentobarbital sodium (12.5mg/ml) in 0.9% NaCl. Upon confirmation of deep anesthesia, a midline incision was made in the abdomen. Then the heart was exposed and a small incision made in the right auricle. Immediately a solution of 4% glutaraldehyde in 0.1 cacodylate buffer (pH 7.2-7.4) was delivered through the apex of the left ventricle over a period of 8 min. Fixative was perfused at estimated physiological pressure, using an apparatus designed to monitor delivery pressure. In animals in which vascular permeability was studied, horseradish peroxidase (HRP, 300 mg/kg) was injected via the jugular vein and allowed to circulate for 30 minutes prior to transcardiac perfusion. Fixation post dissection, was by immersion overnight in 4% glutaraldehyde in 0.1 M cacodylate buffer at 4°C. Central nervous system regions embedded for electron microscopy included thalamus, cerebellum, brain stem and spinal cord. Tissue being prepared for paraffin embedding was fixed in a buffered paraformaldehyde solution. Following overnight fixation, the brain was sectioned coronally and some sections were immersed in the fixative prior to paraffin embedding and light microscopic examination using sections stained with hematoxylin and eosin (H&E). To identify mast cells, special stains such as acidic toluidine blue and safranin/alcian blue were used.

GFAP-immunostains. Brains were removed from symptomatic transgenic mice aged 6 months of age (n=3) or age matched non-transgenic littermates and fixed overnight in ice-cold 4% buffered paraformaldehyde and embedded in paraffin. Sections (5 μm) were processed according to standard procedures. Slides were blocked with goat serum (Vector, Burlingame, CA) and were incubated overnight at 4°C in a rabbit primary antibody against cow GFAP (DAKO, Carpinteria, CA; diluted 1:2000). Antibody labeled cells were detected

Figure 1. (Opposing page) Histologic findings in GFAP-IL3 mice aged five to six months. **A.** Hematoxylin and eosin stained paraffin section of wild type (control) mouse cerebellum showing normal appearing grey and white matter (Magnification x 100). **B.** GFAP-IL3 mouse cerebellum with massive focal accumulation of macrophages in the white matter from an animal aged five and a half months (Magnification x 300). **C.** Paraffin section stained with acidic toluidine blue to identify mast cells in a wild type (control) mouse. This saggital section includes areas of cerebellum (left), diencephalon and brain stem. Few mast cells are seen (magnification x 100). **D.** Numerous mast cells appear in the diencephalic region of a GFAP-IL3 mouse. In the lower part of the picture cerebellar mast cells are also prominent (magnification x 100). **E.** At higher magnification (x 300), mast cells are seen between cerebellar folia and on the brain surface. F. One micron thick sections stained with methylene blue azure II, showing partially degranulated mast cells among intact myelinated fibers and in areas populated with neurons (Magnification x 300). **G.** Electron micrograph showing an intraparenchymal mast cell from affected cerebellar white matter. Cell processes touch a small demyelinated axon which is flanked by a macrophage (m). There is extensive gliosis and lipid deposits are scattered through the tissue. Magnification x 5850. **H.** Mast cell from a demyelinated area. Fine punctate densities (arrowhead) are characteristic of in situ degranulation. Empty cavities are lined by amorphous lightly staining material, possibly lipid (L). Magnification x 8750.

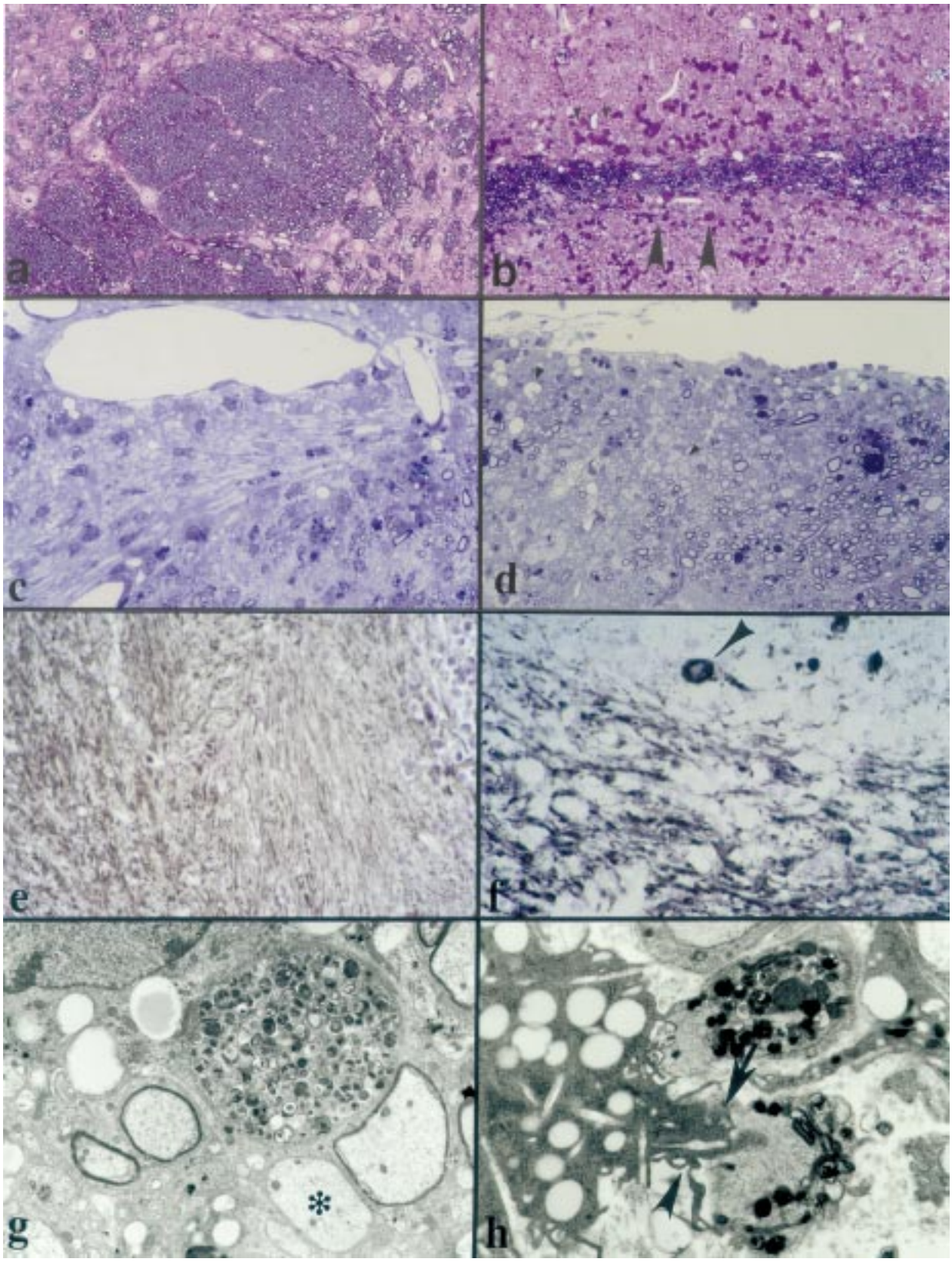
a
b
c
d
e
f
g
h

with an ABC kit (Vector) used according to the manufacturer's instructions.

Astrocyte proliferation studies. For astrocyte proliferation studies, mice were injected intraperitoneally with [^{3}H]-thymidine (2 mCi/g of body weight) ([^{3}H]-methyl-thymidine, Amersham) in 0.5 ml of saline and were killed 4 h after injection by cervical dislocation. Brains were removed, immersion fixed in ice-cold 4% paraformaldehyde, processed and immunostained for GFAP protein as described above. After staining, the sections were dehydrated through a series of graded alcohol solutions and air-dried. Slides were then coated with film emulsion (Type NTB3, Eastman Kodak, Rochester, N.Y.) and placed in a light tight box at 4°C for 4 weeks. The emulsion was developed in DEKTOL (Eastman Kodak) fixed, and counterstained with Mayer's Hematoxylin solution (Sigma).

Immunostaining for axonal abnormalities. To analyse axonal integrity, adjacent sections to those used above for the GFAP immunostains were blocked with goat serum (Vector) and then incubated overnight at 4°C in a mouse monoclonal antibody cocktail against phosphorylated neurofilaments (SMI-312; Sternberger Monoclonals Incorporated, Baltimore, Md). After washing, sections were incubated for 60 min at room temperature in biotin-conjugated rat anti-mouse Ig (diluted 1:400; Southern Biotechnology Associates, Birmingham, Al) followed by washing and incubation for 60 min at room temperature in peroxidase-conjugated strepavidin (diluted 1:2000; Boehringer-Mannheim, Indianapolis, In). Staining employed 3'3'diaminobenzidine (Sigma) as substrate. Prior to mounting, sections were counterstained with Mayer's hematoxylin, and dehydrated in graded ethanols.

Electron microscopy and immunolocalization. Asymptomatic mice aged four months (n=3), symptomatic mice aged 5-6 months (n=6) and control (n=4) were used for electron microscopy. Additional symptomatic animals (n=2) were perfused with HRP in order to visualize changes in vascular permeability. To prepare tissue for EM one millimeter cubed blocks were post-fixed in a 1% aqueous osmium tetraoxide solution for 2 hours, dehydrated using a graded series of ethanols and propylene oxide and infiltrated with resin. The resin mixture contained a 1:1 ratio of propylene oxide and after four hours of exposure, was replaced with 100% araldite. Overnight fixation was followed by embedding in fresh araldite resin. One micron thick sections were cut with glass knives and stained with paraphenylene diamine (PPD) or methylene blue azure II in preparation for light microscopic examination. These sections were used to survey the tissue for lesions prior to sampling blocks for EM.

After fat staining revealed lipid accumulation in glia as well as in macrophages, electronmicroscopy with immunogold labelling was used to confirm astrocyte uptake of fat. Immunogold labelling for ultrastructural visualization of glial fibrillary acidic protein was also performed on tissue embedded in appropriate resins, lowicryl and LR white. Tissues fixed in phosphate buffered paraformaldehyde were dehydrated in a graded series of ethanol, followed by two hours in 50:50 ethanol and L R White methacrylate resin and 24 hours in 100% resin. All reagents were precooled and maintained in an ice water bath. Resin and tissue filled Beem capsules were placed in 60 deg. oven and polymerized for 24 hrs.

An additional group of tissues were post fixed in osmium tetroxide and embedded in polybed 812-araldite epoxy resin followed by oven polymerization for two days. All samples were cut at 0.5 microns and

Figure 2. (Opposing page) Demyelination and axonal changes: immunocytochemistry SMI-312. **A.** Intact brainstem white matter in a presymptomatic mouse. Note the compact appearance of white matter tracts. Original magnification x 300. **B.** Cerebellar white matter from a presymptomatic mouse, four months of age. The white matter is intact, but mononuclear/microglial cells are prominent in the surrounding neuropil (arrowheads). Original magnification A-F x 300. **C.** One micron thick plastic sections confirm the presence of perivenular demyelination in this section taken from the brainstem. **D.** Transverse section of brain stem from a symptomatic GFAP-IL3 mouse at illustrating demyelination in brainstem white matter in a symptomatic mouse, five months of age. Demyelinated axons are seen in cross section (arrowheads). **E.** SMI-312 staining in the cerebellar white matter of a wild type (control) mouse. Note the uniform light staining of the axons. **F.** White matter stained with SMI-312 from a symptomatic mouse. Heavily stained axonal profiles are apparent consistent with dystrophic alterations. A dystrophic neuron (arrow) is seen, upper center. **G.** Electron micrograph showing affected white matter containing a demyelinated axon (*) and a thinly myelinated axon next to it. At the center of the picture there is a greatly swollen axon, filled with darkly staining organelles. This profile is characteristic of Wallerian degeneration. Magnification x 6000. **H.** Macrophage processes infiltrate dystrophic axons. Finger like cytoplasmic extensions of the macrophage (arrowheads) intrude into the axonplasm each of these abnormal axons in which electron dense lysozomal type inclusions signify Wallerian degeneration. Portion of an intact but thinly myelinated axon is seen (above center) adjacent to the dystrophic axons; the unusually thin myelin sheath is characteristic of remyelination. Magnification x 10,000.

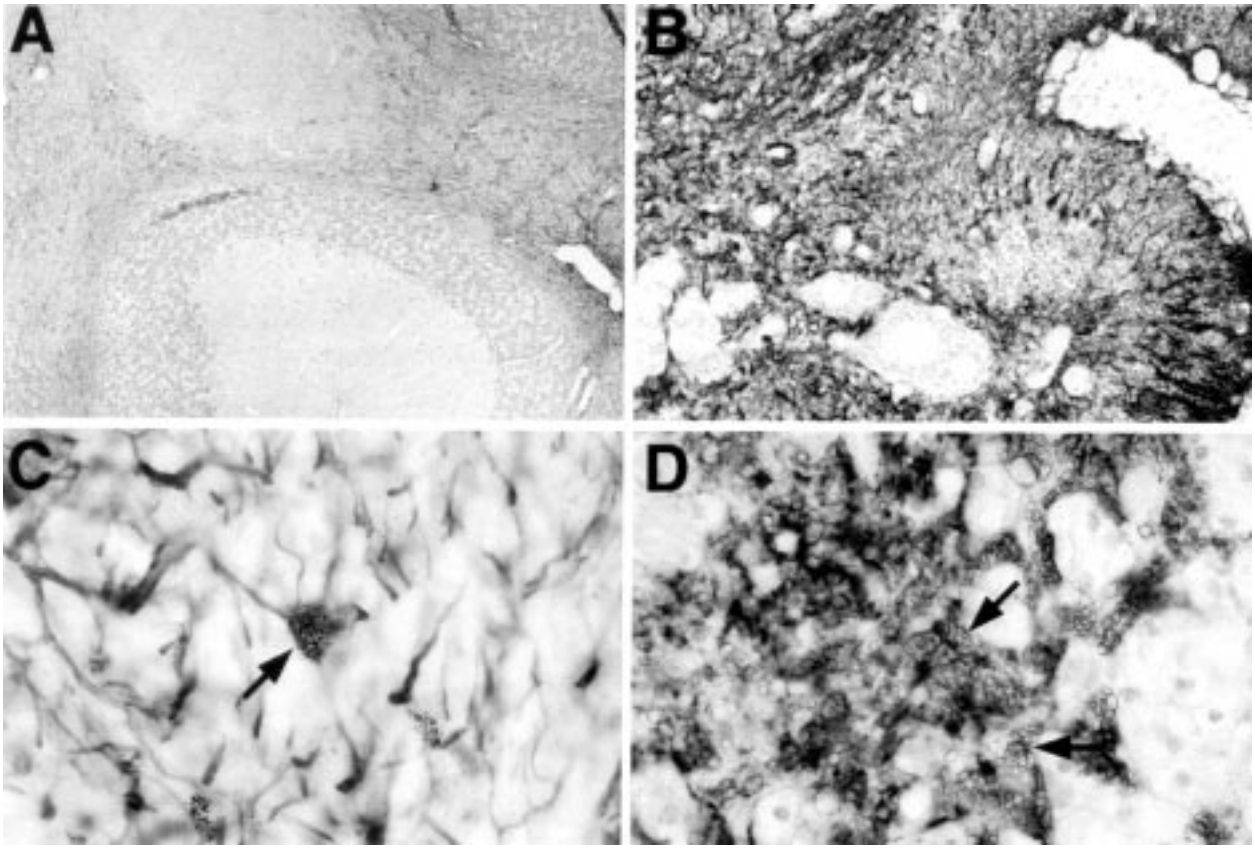

Figure 3. Immunostaining for GFAP. **A.** Cerebellar white matter from control mouse brain. Gray and white matter show only background staining. **B.** Compared to the control tissue, this section from a cerebellar lesion shows pronounced astrogliosis of white matter. **C.** GFAP-IL3 positive astrocytes co-labelled with tritiated thymidine consistent with proliferative activity. **D.** Astrocyte participation in the phagocytic process is evident in this GFAP immunopositive cell that also contains lipid vacuoles. (Original magnification A,B,C,D x 300).

stained with toluidene blue and examined microscopically. Sections selected for ultrastructural analysis were cut at 60nm and those selected for immunolabeling were cut at 100nm. All samples were placed on copper or gold grids and stained with uranyl acetate and bismuth subnitrate.

For immunolabeling ultrathin LR White, grids were incubated in 1% aquaeous sodium borohydride for 15 mins to neutralize reactive aldehyde groups. Following distilled water rinsing, sections were conditioned in PBS containing 2% bovine serum and normal goat serum for half hour. After decanting, grids were incubated for one hour in the above medium containing 1: 1000 dilution of rabbit antibody to GFAP obtained from Sigma Chemical Co. Following PBS rinsing sections were incubated in 1:50 goat anti rabbit colloidal gold (Sigma) for 1 hour. After rinsing in PBS and distilled water, grids were stained as described above. Sections consisting of epoxy resin were first etched in 0.1% sodium ethoxide for 2 mins, rinsed in distilled water and incubated in 1% aqueous sodium metaperiodate to remove osmium prior to viewing in the electron microscope.

Vascular permeability. The procedure for tissue processing differed when altered vascular permeability was being studied. To facilitate the histochemical reaction vibratome sections were cut at a thickness of 50 mm. These sections were then washed in Tris buffer (pH 7.4) and preincubated with diaminobenzidine (DAB; 1mg/ml) for one hour followed by transfer to DAB containing hydrogen peroxide (0.0025%) for 30 minutes to visualize the HRP (32). Selected sections were then washed in buffer, postfixed in osmium tetraoxide and embedded in resin. Semi-thin resin sections stained with 0.1% toluidine blue in borate buffer were used to identify vessels for subsequent study by electron microscopy. Ultrathin sections (70 nm) were then cut on a Sorvall MT 6000 Ultramicrotome with a diamond knife and

placed onto uncoated grids (Gilder grids G200H5) cleaned with acetone. Thin sections, unstained to facilitate HRP recognition, as well as regularly stained thin sections were then examined by EM. The latter were stained with uranyl acetate and bismuth subnitrate.

Results

Histological features. White matter lesions in symptomatic animals appeared in the cerebellum (Figure 1A, B) and brain stem and consisted of focal accumulations of macrophages. Myelin stains of this material showed macrophages with myelin debris in their cytoplasm and plastic sections stained with methylene blue azure II revealed demyelinated axons and foamy macrophage filled with lipid and membranous debris. These changes were seen in animals at five and a half months of age. Paraffin sections stained with H&E from presymptomatic animals aged four months showed no overt pathologic changes. One micron thick sections of araldite embedded tissue appeared normal with rare exceptions in which perivascular and intraparenchymal macrophages were noted. Lymphoid cells were not seen at these time points, however staining for mast cells was positive in the five month old symptomatic mice, with particularly large numbers of these cells appearing in the thalamus (Figure 1C-F). Mast cells were seen in other sites, but were most numerous in the diencephalon and meninges (Figure 1D, F) and were less prominent in demyelinated regions, possibly because of degranulation. Using metachromatic stains, mast cells could be seen in and around blood vessel walls. In contrast to the marked infiltration in GFAP-IL3 mice, very few mast cells were observed in wild type controls (Figure 1C) and these cells were limited to the diencephalon and meninges. Mononuclear cells and macrophages filled with crystalline intracytoplasmic inclusions, were seen on the surface of the cerebellar parenchyma and surrounding blood vessels (Figure 2B, D; Figures 5, 6). Throughout the affected area lipid deposits were scattered within the brain parenchyma. These were identified by fat stains (Figure 3D) and in plastic embedded sections (Figures 4 A-C, 5B, 6C). Cystic degeneration and collapse of the white matter occurred in areas of exceptionally severe activity (Figure 6A, B). In addition to cerebellum and brainstem, similar inflammatory changes, appeared in the spinal cord. As in the cerebellum, spongy degeneration of myelin was found in the white matter. Plastic sections also revealed evolving myelin abnormalities such as swelling and lysis of myelin sheaths. In the same sections there was evidence of phagocytic activity and multinucleate macrophages were seen as well as mononuclear cells and macrophages engorged with myelin debris (Figures 5, 6). In the spinal cord demyelination and macrophage infiltration were prominent in the posterior columns of white matter. Both demyelination and Wallerian degeneration appeared in the lateral columns. Inflammation was also detected in the eye where the cornea, lens, iris, uveal tract and retina were all involved (12, 46). These changes extended to the optic nerve (46).

Astrocyte abnormalities. Astrocyte changes were notable, with GFAP immunostaining revealing a pronounced astrogliosis involving lesion areas within the cerebellum (Figure 3B). In addition to hypertrophy, accumulation of astrocytes within and surrounding lesion areas was due in part to proliferation of these cells indicated by GFAP-immunopositive cells that co-labelled with ^{3}H-thymidine (Figure 3C, arrowed). A marked phagocytic response by astrocytes was also noted with numerous GFAP-immunopositive cells that contained neutral fat vacuoles (Figure 3D, arrowed) scattered throughout affected white matter in the cerebellum. The association between gliosis and lipid accumulation was also apparent in resin embedded tissue prepared for electron microscopy. Immunogold labelling with GFAP was used to identify intracytoplasmic filaments within glial cells with fat deposits at the ultrastructural level (Figures 4A-D). Deposits of lipid were scattered through the neuropil as well as being in the cytoplasm of macrophages. Lipid droplets, recognized by their spherical electron-lucent profiles were present in astrocytes (Figures 4B-D) and the identity of these lipid containing glial cells was confirmed by immunostaining at the light microscopic level and by immunogold labelling of their characteristic filaments in appropriately prepared ultrathin sections (Figures 3, 4).

Vascular permeability. Electron microscopic examination provided further insights into the inflammatory process associated with demyelination and tissue destruction. As distinct from controls (Figure 5A), parenchymal tissue from affected mice was infiltrated by mononuclear cells and macrophages. Mononuclear cells attached themselves to the endothelial surface and both mononuclear cells and macrophages were present in the perivenular interstitium (Figure 5B). Macrophages were recognizable by their lysozomal inclusions and many of them contained lipid vacuoles (Figure 5B).

EM was used to demonstrate altered vascular perme-

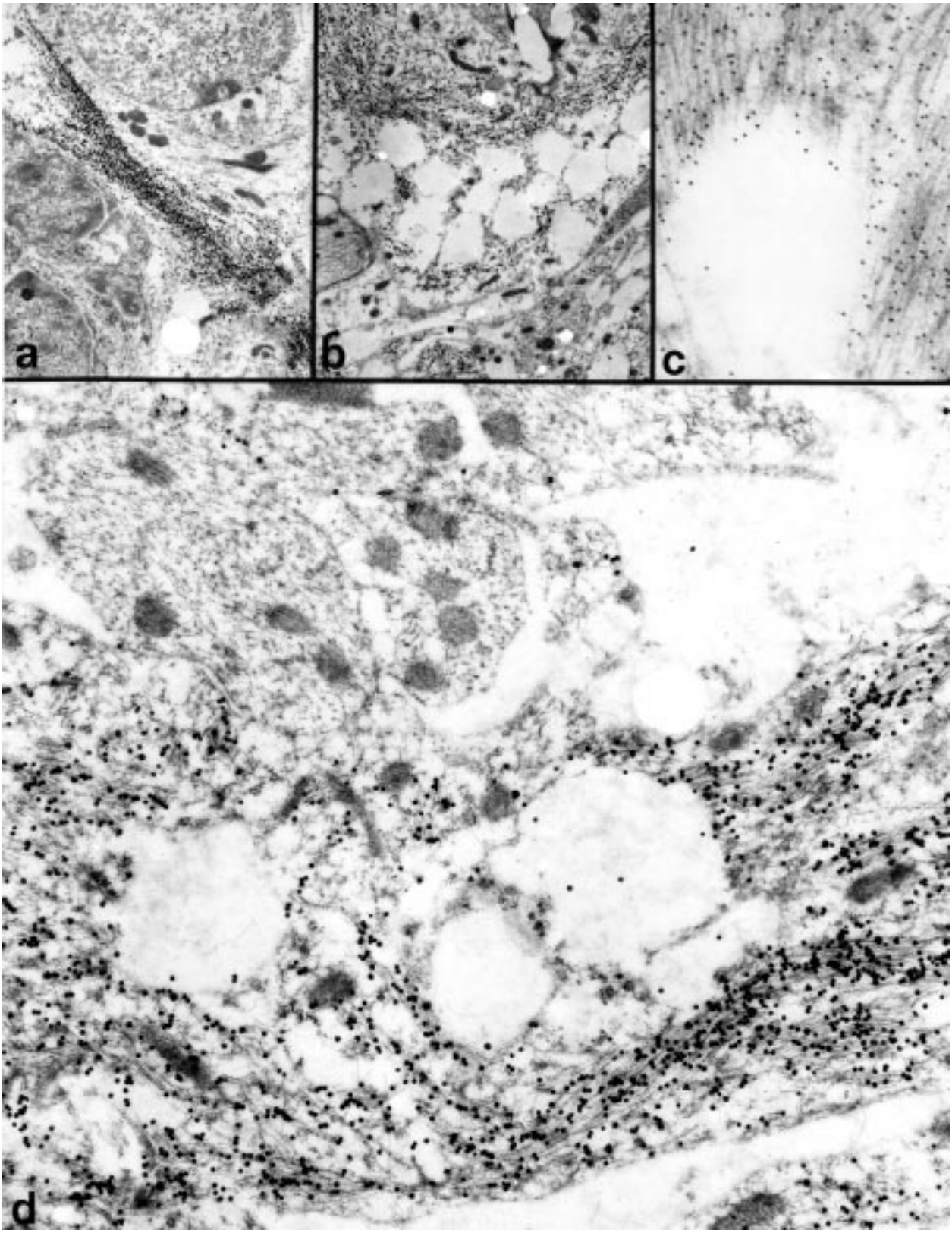
a
b
c
d

ability in brains from animals that received intravenous injections of HRP prior to sacrifice. In wild type mice, reaction product was confined to the vascular lumens (Figure 5C). In order to visualize the HRP reaction product, ultrathin sections prepared for electron microscopy were not stained with uranyl acetate and lead citrate as were other sections used for EM. In symptomatic G3C2 mice at 5.5 months of age, focal extravasation of HRP (Figure 5D) was observed into areas with inflammatory demyelination. Despite the active leakage, neither abnormalities of vascular tight junctions nor endothelial fenestrae were detected and vessel structure appeared normal.

Mast cells. Mast cells were observed on the surface of the brain, around blood vessels and throughout demyelinated lesions (Figure 1C-F). Most numerous in the thalamus, they were less conspicuous in light micrographs of demyelinated regions. However electron microscopy detected degranulating cells in regions of active demyelination. They were identified by their large populations of homogeneous appearing electron dense granules and distinctive surface folds. Partially degranulated mast cells (Figure 1G-H) were observed in cerebellar and brain stem lesions as well as cells containing lipid droplets and membranous debris consistent with phagocytic digestion (Figure 1F). These paracrine cells were found in brain tissue in areas with inflammatory demyelination and gliosis. Surfaces on which they appeared were often lined by basal lamina. This lining could be distinguished from basal lamina constituting the glia limitans. Collagen fibrils also were noted in the vicinity of mast cells. While conspicuous, mast cells were greatly outnumbered by macrophages many of which were filled with crystalloid inclusions. These distinctive inclusions have been described elsewhere (10, 47).

Demyelination and oligdendrocyte changes. Demyelinated axons were observed (Figures 2B, 6A-F), as well as many axons that were enveloped by abnormally thin myelin sheaths, characteristic of remyelination. Swelling and lysis of myelin sheaths was observed in cerebellar and brainstem white matter. Dystrophic axons were detected both by immunostaining with SMI-312 (Figure 2C-F) and by electron microscopy (Figure 2 E, F). EM showed macrophages apparently engaged in phagocytosis of dystrophic axons (Figure 2F). As indicated above demyelination was seen throughout affected areas (Figures 2G; 6A,B). Demyelinated axons were commonly found in the brainstem (Figure 6C) and thinly myelinated axons characteristic of remyelination were also observed. Consistent with widespread demyelination, oligodendroglial cells showed proliferative changes. These cells could be recognized by their myelin plasmalemmal connections (Figure 6D-F) and connections to several remyelinating axons were observed in sections through a single cell. Myelin plasmalemmal connections formed either at the surface of the cell or arose within the cytoplasm (Figure 6D). Remyelinated axons were sometimes enveloped by spiral processes extending from the oligodendrocyte (Figure 6E). The oligodendroglial cytoplasm was ample, with abundant organelles and numerous microtubules in the cytosol. Organelles included mitochondria, rough endoplasmic reticulum and golgi apparatus. Lysozomes were prominent and often packed with paracrystalline profiles of variably electron dense material. These inclusions were round, oblong, elliptical or crescent shaped. Evidence of phagocytosis by oligodendroglia consisted of membrane enclosed lamellar debris (Figure 6E) and lysozomal inclusions (Figure 6F).

Discussion

Resident CNS cells appear to play a significant role in the pathogenesis of demyelination observed in the GFAP-IL3 mice; findings consistent with previous observations in human inflammatory demyelinating disease (31). However, unlike inflammatory demyelination observed in other experimental models, the destruction of myelin occurring in these animals involves activated microglia, infiltrating monocuclear cells, with an additional phagocytic role for astrocytes which were filled with lipid (Figures 3, 4). The demyelinating lesions consisted of discrete focal inflammatory infiltrates resembling plaques (Figure 1A, B). Some aspects of the inflammatory demyelination in these animals are noteworthy. First, lymphocyte involvement is confined to the late stages of disease (IL Campbell unpublished observations), and therefore the appearance of these cells is a

Figure 4. (Opposing page) Immunogold labelling for GFAP. **A.** Immunogold labelling accentuates the shrunken gliotic cerebellar white matter in this electron micrograph. Original magnification x 6200. **B.** A cluster of lipid droplets surrounded by immunolabelled glial filaments. Original magnification x 8000. **C.** Higher power electron micrograph showing a single lipid vacuole enveloped by immunolabelled glial filaments. Lipid vacuoles conspicuously present in glial cytoplasm fail to immunostain as do organelles such as mitochondria. Original magnification x 24,000. **D.** Demyelinated axons and lipid droplets both fail to stain, but intracytoplasmic filaments stain intensely with GFAP. Original magnification x 25450.

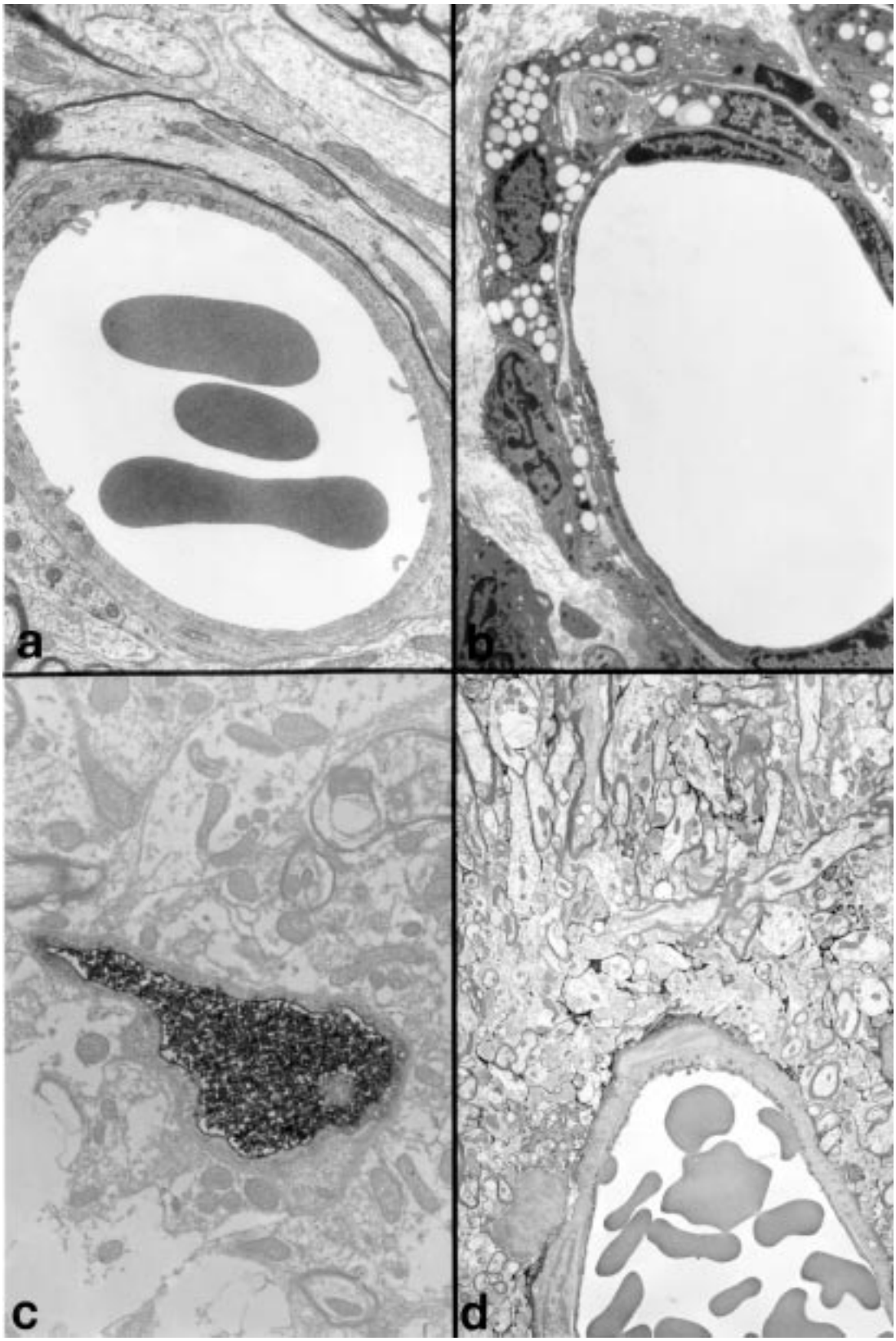
a
b
c
d

secondary phenomenon. The injury appeared directly focused on the myelin sheath (Figures 2B, 6A-F) rather than at oligodendroglial cytoplasm, as these myelin forming cells survived the process of demyelination. Oligodendrocytes appeared to be actively involved in remyelination, being readily identified through their distinctive connections to remyelinating axons (Figure 6C-F). Further evidence of their persistence during the process of demyelination, is the normal staining for CNP-ase in areas of active demyelination reported (12). These myelin forming cells, identified by electron microscopic visualization of their myelin-plasmalemmal connections (30), contained phagocytosed myelin debris (Figure 6D) and compacted electron dense material within organelles (Figure 6 C,E). Thus it appears that like the other glial cells, they take part in the phagocytic process. In the following paragraphs we will discuss 1), the significance of axonal degeneration in this primary demyelinating disease, 2), mast cell degranulation and altered vascular permeability in the initiation of the inflammatory process and 3), the response of oligodendrocytes and astrocytes in phagocytosing myelin debris and lipid droplets.

Axonal degeneration. Axons are vulnerable to changes in their microenvironment and degenerative axoplasmic abnormalities were noted in regions of active demyelination. In addition to removing myelin debris, the cytoplasmic processes of macrophages could be seen infiltrating abnormal axis cylinders (Figure 2H). The presence of widespread axonal dystrophic changes were confirmed by immunostaining with SMI-32 (Figure 2E-F). Axonal injury is not unusual in demyelinating encephalitis, especially in the presence of vigorous inflammation (18, 28, 45, 56, 58). This observation has received considerable discussion recently in studies of axonal injury in MS (56, 58), and is supported by previously reported experimental findings in demyelinating disease occurring in peripheral nerve (18), which call attention to dose-dependent axonal swelling in the sciatic nerves of rats inoculated with peripheral nerve myelin, to induce experimental allergic neuritis. Incidental damage to axons in the course of demyelinating disease is more easily visualised and quantified in the PNS. In pathologic studies of the experimental model allergic neuritis (18, 45) it has been reported that when myelin is the primary target of an immune response, incidental axonal injury is proportional to myelin dosage (18) and to the space occupying effects of inflammatory cells and edema (45), moreover the number of damaged axons reaches its peak when inflammation is most severe and increased tissue pressure is maximum. Due to a paucity of available extracellular space, the neural microenvironment central and peripheral, is vulnerable to the accumulation of cells and fluid associated with the inflammatory process. In the GFAP-IL3 mouse space occupying effects of cells and fluid accumulating within and around brain lesions, may contribute to ischemic and compressive axonal injury.

Mast cells, macrophages and altered permeability. While endothelial cells and astrocytes are well studied elements of the BBB (4, 32) mast cells may also contribute to altered vascular permeability. Although they are found only in a few specific areas of the brain, parenchymal mast cells are located in regions considered more permeable than the rest of the CNS (15). They are also located in the meninges and in both locations these cells are believed to be capable of modulating vascular permeability (42). Mast cells have been implicated in the inflammatory process that occurs in both clinical and experimental demyelination (22, 27, 40), but the role of these cells in inflammatory demyelinating diseases may be somewhat understated (40), since some routinely used histologic stains may not identify them (22, 27). In conditions such as EAE, EAN and in the GFAP-IL3 mouse, use of appropriate metachromatic stains and electron microscopy, can help illustrate the presence and activity of these immunoeffector cells (42, 55). For this reason, studies reporting increased mast cell activity in multiple sclerosis (27, 40, 55) are of particular interest and demonstration of mast cells in both MS and experimental models such as EAE and GFAP-IL3 mice suggests a potentially valuable line of inquiry for continuing research in this field (12, 42, 57). Studies with nuclear magnetic resonance reveal that altered vascular permeability may occur in MS lesion sites (26, 41). Mast cell traffic (Figure 1 C-G) is sub-

Figure 5. (Opposing page) Vascular abnormalities. **A.** Electronmicrograph illustrating a normal appearing capillary in white matter from a control mouse. The adjacent perivascular space contains several intact myelinated fibers. Magnification x 8000. **B.** Perivenular macrophages in GFAP-IL3 mouse white matter. Many of them are filled with lipid inclusions. Slender linear inclusions are present in the macrophage in the upper right corner. Magnification x 3857. **C.** Unstained section showing horseradish peroxidase reaction product in an intact vessel from unaffected brain tissue in a GFAP-IL3 mouse. Magnification x 11,100. **D.** Unstained section from the white matter lesion site in a symptomatic mouse with demyelination. HRP reaction product fills the perivenular parenchyma. Magnification x 4000.

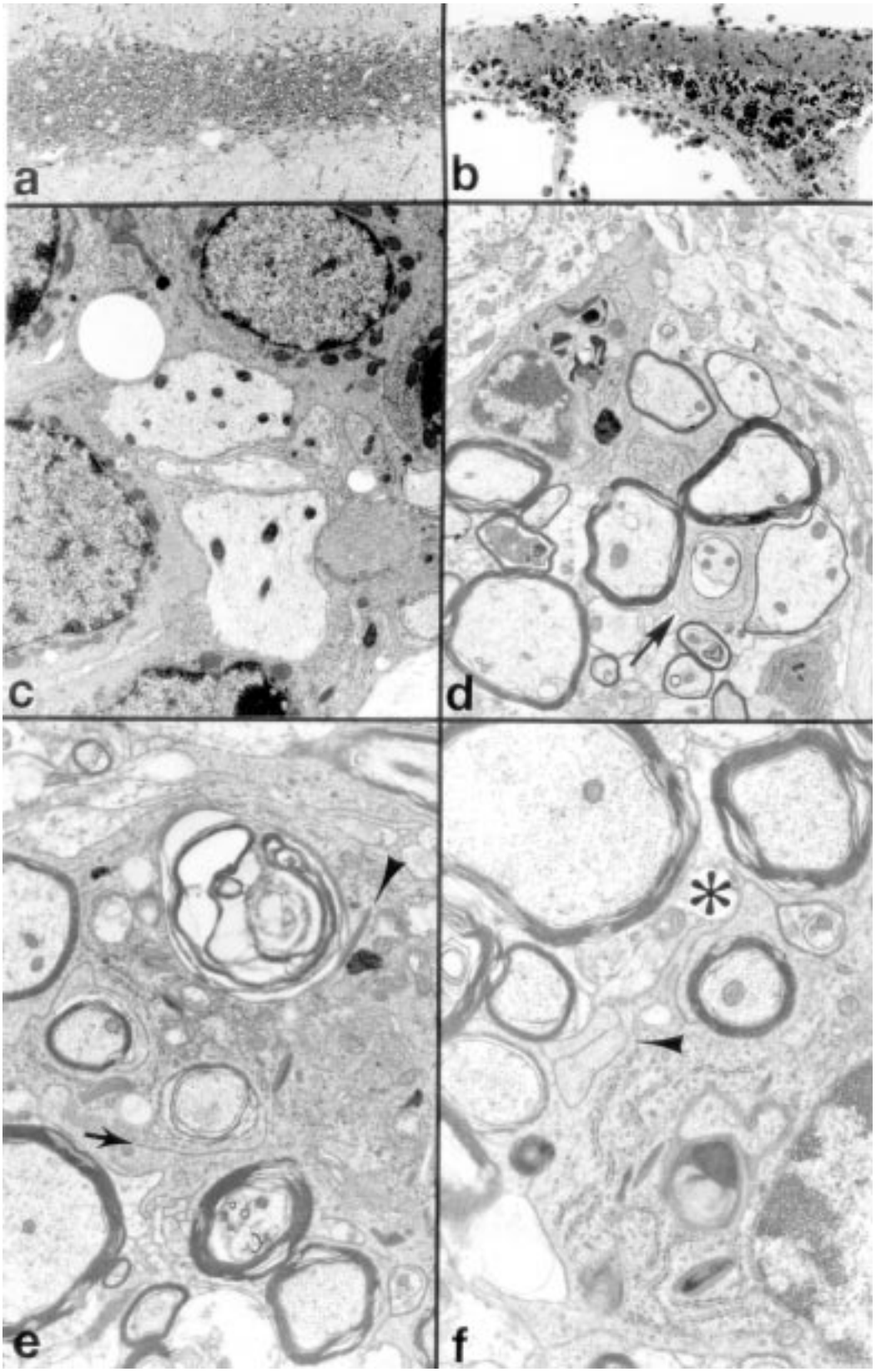
a
b
c
d
e
f

stantially increased in GFAP-IL3 mice, probably in response to the cytokine (50). Their presence at the lesion site may facilitate local permeability changes, as demonstrated here, and help promote macrophage infiltration. Continued release of histamine and other bioactive substances by degranulating mast cells, may serve to maintain altered permeability facilitating cellular traffic to and from the neural microenvironment. Structural interaction between mast cells and other cell types have been described (15), including 'transgranulation' and 'pseudopod translocation' (17), whereby mast cells can transfer their granules to adjacent cells including macrophages. Since mast cells are far less numerous than macrophages such interactions might amplify the mast cells capacity to alter vascular permeability. Furthermore the ability of mast cells to release proteases that digest myelin basic protein (MBP) may either initiate or reinforce the process of demyelination (23, 55), since mast cells respond to MBP (23). While mast cells were originally classified as paracrine secretory cells, their role is now interpreted more expansively, as evidence accumulates that they are involved in phagocytosis (44) and that they process antigens from phagocytosed material (37). Mast cells can degranulate explosively in anaphylactic states (global degranulation) or, more slowly, in a graded or 'piecemeal' fashion, in proportion to the degree of injury (16). In the present study, partially degranulated mast cells were encountered in sections stained with metachromatic dyes (Figure 1F) and EM showed granule bearing cells with lipid material and membrane bounded intracytoplasmic debris. It is of interest that these cells may degranulate in the presence of myelin basic protein and can induce demyelination in vitro that is greatly augmented by estradiol (54). The latter is noteworthy in view of observations that female mice with the GFAP-IL3 transgene show earlier onset of disease, succumbing at 130 days of age while male counterparts do not become symptomatic until 150 days of age and that pregnancy exacerbated the process further (12). The relationship of mast cells and gender is discussed more fully elsewhere (15).

Interaction between macrophage/monocytes and the BBB may also contribute to alterations of the vascular endothelium that may result in increased permeability (for review see Perry and associates 44). Macrophages are known to produce a range of mediators that could potentially modify the function of the vascular endothelium, in particular the cytokines IL-1b and TNF-α (13) and the matrix metalloproteinases (MMP, for references see Chandler et al. 11). Expression of these mediator genes is increased in the CNS of the symptomatic GFAP-IL3 mice (11 and 43). However in spite of this increase in cerebral IL1-α and TNF-α gene expression, in recent experiments (unpublished) we failed to observe increased vascular expression of the cellular adhesion molecules ICAM-1, VCAM-1 and MAdCAM. This finding does not support a cytokine mediated activation of the endothelium and suggests other pathways (e.g. MMP) are more crucial to the development of altered BBB permeability in GFAP-IL3 mice.

Macrophages and activated microglial cells are far more numerous than mast cells in the inflammatory lesions in the GFAP-IL3 mouse. Their predominance as well as the absence of lymphocytes from the initial lesions are at variance with the concept of demyelinating disease orchestrated by lymphocytes, in which macrophages may be viewed as playing a subsidiary role. Of course this view owes much to the influence of classic models such as experimental allergic encephalomyelitis; however even in EAE there is good evidence that macophages play a central role in the demyelinating phase of the disease (5, 20). There are indications also of macrophage predominance in human demyelinating disease. Although human neuropathologic studies of MS have been hampered by scarcity of autopsy material, valuable tissue from active disease may become available when rapidly enlarging CNS lesions are biopsied. In these situations surgical explo-

Figure 6. (Opposing page) Demyelination. **A.** One micron thick section through a cerebellar folium showing the compact appearance of normal white matter. Magnification x 300. **B.** One micron thick section stained with toluidene blue showing cystic degeneration of cerebellar white matter as well as dense infiltration by macrophages at the gray-white junction. Macrophages can also be seen infiltrating the leptomeninges and penetrating the cerebellar cortex. Magnification x 300. **C.** Demyelinated axons near the parenchymal surface of the brain stem. Magnification x 8400. **D.** Demyelinated, remyelinating and myelinated axons adjacent to a vessel (upper right). The cell at the center of this illustration is an oligodendrocyte, and shows myelin-plasmalemmal connections (arrow) to two remyelinating fibers (lower center). The oligodendroglial cytoplasm contains electron dense debris compressed into paracrystalline and spheroid bodies. Magnification x 6500. **E.** Another oligodendroglial cell showing plasmalemmal attachments to several myelinated fibers. Note the large membrane bounded inclusion with lammelar debris undergoing phagocytosis. A crystalloid structure appears to fuse with the degenerating myelin (arrowhead). Magnification x 6667. **F.** In this oligodendrocyte different configurations of the myelin plasmalemmal connection can be observed. The connection may arise from the cell surface (asterisk) or deep inside the cytoplasm (arrowheads). There are microtubules within the cytoplasm and there are paracrystalline deposits of autophagic material. Magnification x 16,000.

ration is carried out because the clinical presentation of aggressive lesions can mimic the presentation of fast growing tumors (7, 21, 24, 25, 38). Pathologic samples obtained from active lesions biopsied because of suspected tumor, are often overwhelmingly populated with macrophages (20, 24, 38) leading some authors to indict the macrophage (51) as the 'villain' in the pathogenesis of MS.

Response of oligodendroglia and astrocytes. Clinical and experimental studies have shown that demyelination may be the consequence of either injury to the myelin producing oligodendrocyte or, the result of direct damage to the myelin sheath, or a combination of the two. Since Lumsden (33) drew attention to the loss of oligodendrocytes in human MS, experimental models for oligodendroglial and myelin injury have received increased interest from investigators. Oligodendroglial injury may occur through the cytolytic properties of viruses (30) or toxins (34, 35, 36). Alternatively myelin may present a direct target to immune attack, as in EAE or in specific forms of neurotoxic injury (29, 34). Since oligodendrocytes are the myelin forming cells in the CNS, it is important to study the behaviour of these cells in models of demyelination and also to determine whether affected cells are capable of remyelination. In contrast to viral and toxic models of myelin injury, immune mediated demyelination is a more complex process (31, 32, 33, 34, 35) since a variety of effector cells and soluble mediators appear to be involved. To address this problem new models are necessary to evaluate each effector mechanism independently (9, 10).

The growing attention to cytokines has provided new paradigms for demyelinating injury (3, 6, 9, 10, 31, 34). Insights into the behaviour of cytokines come from immune models of demyelination and from transgenic models in which specific cytokines are expressed (52, 53, 57). The advent of these models has also supported the view (31) that indigenous cells of the CNS, as well as infiltrating cells, may be actively involved in the process. Both macrophages and mast cells may secrete proteases (22, 23, 52, 53, 57) and cytokines, such as TNF-α which is released by degranulating mast cells and can damage myelin (15, 52, 53), thereby attracting macrophages to the site of tissue injury. Recent clinical and experimental evidence provide support for the view that activated macrophage/microglia play a critical role in the evolution of chronic inflammatory demyelinating disease (3, 6, 52, 53,57).

In addition to secreting certain cytokines themselves, astrocytes appear to be involved in other aspects of the disease process. These cells express MHC Class II antigens and other markers consistent with involvement in inflammatory/immune processes (31, 39). From the initial phase of the disease in which altered permeability occurs (Figure 5), to the later stages in which glial scarring takes place these cells appear to be continually involved. The demyelinating lesions observed in the GFAP-IL3 animals were accompanied by severe gliosis (Figures 5, 6) and lipid accumulation in reactive astrocytes (Figures 3, 4). Evidence of the latter phenomenon was further supported by electron microscopic visualization of lipid droplets in sections stained with immunogold labeled antibody to GFAP (Figure 3). Astrocyte responses to injury include both pinocytosis and phagocytosis (39); furthermore these glial cells contain APO E which appears to be involved in removal of lipids accumulating after injury (2). Certain astrocytic neoplasms such as xanthogranulomatous astrocytomas are known to contain abundant lipid (19, 24) and lipidized glioblastomas have been described. Because the phagocytic potential of astrocytes has received somewhat less attention than other properties of these versatile cells, we sought to illustrate it through appropriate fat and glial staining (Figures 3, 4). Glial scarring in which affected cells show filament accumulation is a commonly observed glial response to injury and may be the consequence of a wide range of noxious stimuli; physical, chemical, immune and metabolic (for review see ref 39). The vigorous glial responses observed here are consistent with severe inflammatory demyelinating disease, of greater severity than chronic multiple sclerosis in which gliosis appears in perivenous locations (1).

Active inflammatory demyelinating disease may affect cranial nerves and the eye (14, 46). Cranial nerve palsies and retinal inflammation have been detected during the initial phase of multiple sclerosis and are associated with active disease. It is of interest therefore that severe inflammatory changes have been encountered in the retina and optic nerves of symptomatic GFAP-IL3 mice (46). These changes are associated with mast cell proliferation and degranulation in the retina, choroid and iris. Hearing loss has also been detected in GFAP-IL3 mice (Woolf personal communication) and abnormal brainstem auditory evoked responses documented. Inflammation in the vicinity of the cochlear nucleus and damage to the cochlear branch of the VIII nerve were noted in affected animals. Interestingly demyelinating disease accompanied by vigorous inflammation and SMI-312 positive axons in and around the cochlear nucleus appeared concurrently with Wallerian degeneration in the spiral ganglion in animals with complete hearing loss.

Conclusion

The GFAP-IL3 mouse provides an example of inflammatory demyelination unrelated to classical autoimmune, viral or toxic etiology; instead the disease is induced by chronic expression of a specific cytokine and the cells and molecules under its influence. The model facilitates study of the response of resident cells such as astrocytes, oligodendroglia, microglia and mast cells as well as the infiltrating cells of hematogenous origin. Degranulation of mast cells noted in lesion areas, is consistent with a mast cell role in the pathogenesis of altered vascular permeability, a mechanism that has been implicated in the earliest stage in the pathogenesis of new lesions in multiple sclerosis (26, 41). Increased mast cell activity occurring in MS brains (22, 27) may facilitate infiltration of inflammatory cells into brain parenchyma. In the GFAP-IL3 mouse, mast cell infiltration and degranulation are temporally associated with increased vascular permeability to macromolecular tracers such as HRP. The potential value of this transgenic model for neuropathologic investigation derives from the following: 1) the neuropathologic findings provide insights into macrophage predominant demyelination, increasingly recognized in studies of human material (7, 21, 25, 38); 2) earlier onset in female mice may help elucidate gender-related susceptibility encountered in human MS; 3) astrocyte proliferation and lipid incorporation suggest that these cells may play a supportive role in macrophage mediated demyelination; 4) involvement of the optic nerves as well as other cranial nerves, will facilitate experimental study of MS related complications involving axonal dystrophy; and 5) implication of specific cytokines such as IL-3 and TNF-α in the pathogenesis of demyelinating disease may help further our understanding of the role of these immunomodulators in inflammatory demyelinating disease.

Acknowledgements

The authors thank Jesus Macias for his assistance with photography and Dr Barney Walsh for his help in manuscript and bibliographic organization. We are grateful to Carrie Kincaid and Megan Benedict for maintenance and screening of the GFAP-IL3 transgenic mice.

This work was supported by National Institute of Mental Health grant MH 50426 and by National Institutes of Neurological Diseases and Stroke grant NS 14162 and the Veterans Administration Research Service.

References

1. Allen IV (1980). A histological and histochemical study of the macroscopically normal white matter in multiple sclerosis. In: *Progress in Multiple Sclerosis Research*, Bauer HJ, Poser S, Ritter G (eds.), pp. 340-347, Springer Verlag: Berlin
2. Boyles JK, Pitas RE, Wilson E, Mahley RW, Taylor JM (1985). Apolipoprotein E associated with astrocytic glia of the central nervous system and with nonmyelinating glia of the peripheral nervous sytem. *J Clin Invest* 76: 1501-1513.
3. Bradl M, Linington C (1996). Animal models of demyelination. *Brain Pathol* 6: 303-311
4. Brett FM, Mizisin AP, Powell HC, Campbell IL (1995). Evolution of neuropathologic abnormalities associated with blood-brain barrier breakdown in transgenic mice expressing interleukin-6 in astrocytes. *J Neuropathol Exp Neurol* 54: 766-775.
5. Brosnan CF, Bornstein MB, Bloom BR (1981). The effects of macrophage depletion on the clinical and pathological expression of experimental allergic encephalomyelitis. *J Immunol* 126: 614-620
6. Brosnan CF, Raine CS (1996). Mechanisms of immune injury in multiple sclerosis. *Brain Pathol* 6: 243-257.
7. Burger PC and Scheitauer BW (1993). Inflammatory masses simulating neoplasia. In: *Tumors of the Central Nervous System*. Armed Forces Institute of Pathology. Fascicle X Chp 19 pp 391-411.
8. Campbell IL, Abraham CA, Masliah E, Kemper P, Inglis JD, Oldstone MBA, Mucke L (1993). Neurologic disease induced in transgenic mice by cerebral overexpression of interleukin-6. *Proc Natl Acad Sci USA* 90: 10061-10065.
9. Campbell IL (1995). Neuropathogenic actions of cytokines assessed in transgenic mice. *Int J Dev Neurosci* 13: 275-284
10. Campbell IL, Powell HC (1996). Role of cytokines in demyelination. In: *Methods: A Companion to Methods in Enzymology* 10: 462-477, Academic Press
11. Chandler S, Miller KM, Clements JM, Lury J, Corkill D, Anthony DCC, Adams SE, Gearing AJH (1997). Matrix mettaloproteinases, tumor necrosis factor and multiple sclerosis: an overview. *J Neuroimmunol* 72: 155-161.
12. Chiang CS, Powell HC, Gold LH, Samimi A, Campbell IL (1996). Macrophage/microglial-mediated primary demyelination and motor disease induced by the central nervous system production of interleukin-3 in transgenic mice. *J Clin Invest.* 97: 1512-1524.
13. Claudio L, Martiney J, Brosnan CF (1994). Ultrastructural studies of the blood retina barrier after exposure to interleukin-1β or tumor necrosis factor-α. *Lab Invest* 70: 850-861.
14. Commins DJ, Chen JM (1997). Multiple sclerosis: a consideration in acute cranial nerve palsies. *Amer J Otology* 18: 590-595
15. Dines KC, Powell HC (1997). Mast cells in the nervous system. *J Neuropath. Exp Neurol* 56: 627-640

16. Dvorak AM, Tepper RI, Weller PF, Morgan ES, Estrella P, Monahan-Early PA, Galli SJ. (1994). Piecemeal degranulation of mast cells in the inflammatory eyelid lesions of interleukin-4 transgenic mice. Evidence of mast cell histamine release in vivo by diamine oxidase-gold enzyme affinity ultrastructural histochemistry. *Blood* 83: 3600-3612
17. Greenburg G. Burnstock G (1983). A novel cell to cell interaction between mast cells and other types. *Exp Cell Res* 147:1-13.
18. Hahn AF, Feasby TE, Steele A, Lovgren DS, Berry J (1988). Demyelination and axonal degeneration in Lewis rat experimental allergic neuritis depend on myelin dosage. *Lab Invest* 59: 115-125
19. Hosokawa Y, Tsuchihasi Y, Okabe H, Toyama M, Namura K, Kuga M, Yonezawa T, Fujita S, Ashihara T (1991). Pleomorphic xanthoastrocytoma. Ultrastructural, immunocytochemical, and DNA cytofluorometric study of a case. *Cancer* 68: 853-859
20. Huitinga I, van Rooijen N, de Groot CJA, Uitdehag BMJ, Dijkstra CD (1990). Supression of experimental allergic encephalomyelitis in Lewis rats after elimination of macrophages. *J Exp Med* 172: 1025-1033.
21 Hunter SB, Ballinger WE Jr, Rubin JJ (1987). Multiple sclerosis mimicking primary brain tumor. *Arch Pathol Lab Med* 111: 464-468.
22. Ibrahim MZM, Reder AT, Lawand R, Takash W Sallouh-Khatib S (1996). The mast cells of the multiple sclerosis brain. *J Neuroimmunol* 70: 131-138.
23. Johnson D, Seeldrayers PA, Weiner HL (1988). The role of mast cells in demyelination. 1. Myelin proteins are degraded by mast cell proteases and myelin basic protein and P2 can stimulate mast cell degranulation. *Brain Res* 444: 195-198
24. Kepes JJ, Rubinstein LJ, Eng LF (1979). Pleomophic xanthoastrocytoma: a distinctive meningocerebral glioma of young subjects with relatively favorable prognosis. A study of 12 cases. *Cancer* 44: 1839-1852
25. Kepes JJ (1993). Large focal tumor like demyelinating lesions of the brain: intermediate entity between multiple sclerosis and acute disseminated encephalomyelitis? A study of 31 patients. *Ann Neurol* 33: 18-27
26. Kermode AG, Thompson AJ, Tofts P, MacManus DG, Kendall BE, Kingsley DPE, Mosely IF, Rudge P, McDonald WI (1990). Breakdown of the blood-brain barrier precedes symptoms and other MRI signs of new lesions in multiple sclerosis. Pathogenetic and clinical implications. *Brain* 113: 1477-1489
27. Kruger PG, Bo L, Myhr KM, Karlsen AE, Taule A, Nyland HI, Mork S (1990). Mast cells and multiple sclerosis: a light and electron microscopic study of mast cells in multiple sclerosis emphasizing staining procedures. *Acta Neurol Scand* 81: 31-36.
28. Lampert PW (1969). Mechanism of demyelination in experimental allergic neuritis. Electron microscopic studies. *Lab Invest* . 20:127-138
29. Lampert PW, O'Brien J, Garrett R (1973). Hexachlorophene encephalopathy. *Acta Neuropathol* 23: 326-333.
30. Lampert PW, Sims JK, Kniazeff AJ (1973). Mechanism of demyelination in JHM virus encephalitis. Electron microscopic studies. *Acta Neuropathol* 24: 76-85
31. Lee SC, Moore GWR, Golenwsky G, Raine CS (1990). Multiple sclerosis: a role for astroglia in active demyelination suggested by Class II MHC expression and ultrastructural study. *J Neuropath Exp Neurol* 49: 122-136
32. Lossinsky AS, Vorbrodt AW, Wisniewski HM (1986). Characterization of endothelial cell transport in the developing mouse blood-brain barrier. *Dev Neurosci* 8: 61-75.
33. Lumsden CE (1970). The neuropathology of multiple sclerosis. In: *Multiple sclerosis and other demyelinating diseases. Handbook of Clinical Neurology*, Vinken PJ, Bruyn GW (eds) pp. 217-309. North Holland Publishing Co, Amsterdam
34. Ludwin SK (1989). Evolving concepts and issues in remyelination. *Dev Neurosci* 11: 140-148.
35. Ludwin SK (1992). Oligodendrocytes from optic nerves subjected to long term Wallerian. degeneration retain the capacity to myelinate. *Acta Neuropathol* 84: 530-537
36. Ludwin SK (1994). Central nervous system remyelination: studies in chronically damaged tissue. *Ann Neurol* 36 (Suppl) S143-145
37. Malaviya R, Twesten NJ, Ross EA, Abraham SN, Pfeifer JD (1996). Mast cells process bacterial Ags through a phagocytic route for class I MHC presentation to T cells. *J Immunol* 156: 1490-1496
38. Nesbit RM, Forbes G, Scheitauer BW, Okazaki H, Rodriguez M (1991). Multiple sclerosis: histopathologic and MR/CT correlation in 37 biopsied and three cases at autopsy. *Radiology* 80: 467-474.
39. Norenberg MD (1994). Astrocyte responses to CNS injury. *J Neuropathol Exp Neurol* 53: 213-220
40. Olsson Y (1974). Mast cells in plaques of multiple sclerosis. *Acta Neurol Scand* 50: 611-618
41. Ormerod IE, Miller DH, McDonald WI, du Boulay EP, Rudge P, Kendall BE, Moseley IF, Johnson G, Tofts PS, Halliday AM, Bronstein F, Scaravelli F, Harding AE, Barnes D, Zilkha KJ (1987). The role of NMR imaging in the assessment of multiple sclerosis and isolated neurological lesions. A quantitative study. *Brain* 110: 1579-1616
42. Orr EL (1988). Presence and distribution of nervous system-associated mast cells that may modulate experimental autoimmune encephalomyelitis. *Ann N Y Acad Sci* 540: 723-726.
43. Pagenstecher A, Stalder AK, Kincaid CL, Shapiro SD Campbell IL (1998) Differential expresssion of matrix metalloproteinase and tissue inhibitor of matrix metalloproteinase genes in the mouse central nervous system in normal and inflammatory states. *Amer J Path* 152: 729-741.
44. Perry VH, Anthony DC, Bolton SJ, Brown HC (1997). The blood-brain barrier and the inflammatory response. *Mol Med Today* 3:335-341
45. Powell HC, Myers RR, Mizisin AP, Olee T, Brostoff SW (1991). Response of the axon and barrier epithelium in experimental allergic neuritis induced by autoreactive T-cell lines. *Acta Neuropathol* (Berl) 82: 364-387.

46. Powell HC, Campbell IL (1996). Mast cell changes in opthalmic and white matter lesions associated with over-expression of interleukin-3 in transgenic mice. *Brain Pathol* 6: 356 (abstract).

47. Powell HC, Garrett RS, Muellenbachs A, Campbell IL (1997). Crystalloid inclusions in brain macrophages in experimental demyelination. *J.Neuropath. Exp Neurol* 56: 580 (abstract)

48. Probert L, Akassoglou K, Pasparakis M, Kontogeorgos G, Kollias G (1995). Spontaneous inflammatory demyelinating disease in transgenic mice showing central nervous system expression of tumor necrosis factor α. *Proc Nat Acad Sci USA* 92: 11294-11298.

49. Sasaki K, Iwatsuki H, Suda M, Itano C (1993). Cell death and phagocytosis of haematopoietic elements at the onset of haematopoiesis in the mouse spleen: an ultrastructural study. *J Anat* 183: 113-120.

50. Schrader JW (1986). The panspecific hemopoietin of activated T lymphocytes (interleukin-3). *Annu Rev Immunol* 4: 205-230.

51. Sriram S, Rodriguez M (1997). Indictment of the microglia as the villain in multiple sclerosis. *Neurol*; 48: 464-470.

52. Stalder AK, Powell HC, Masliah E, Pasenstecher A, Ascensio VC, Kincaid C, Benedict M, Campbell IL (1998). An adult onset chronic inflammatory encephalopathy in immune-competent and severe combined immune-deficient (SCID) mice with astrocyte-targeted expression of tumor necrosis factor-alpha. *Amer J Pathol* 153: 767-784

53. Taupin V, Renno T, Bourbonniere L, Peterson A, Rodriguez M, Owens T (1997). Increased severity of experimental autoimmune encephalomyelitis, chronic macrophage/microglial reactivity, and demyelination in transgenic mice producing tumour necrosis factor-alpha in the central nervous system. *Eur J Immunol* 27: 905-913

54. Theoharides TC, Dimitriadou V, Letourneau R, Roznieckl JJ, Vliagoftis H, Boucher W (1993). Synergistic action of estradiol and myelin basic protein on mast cell secretion and brain myelin changes resembling early stages of demyelination. *Neuroscience* 57: 861-71

55. Toms R, Weiner HL, Johnson D (1990). Identification of IgE-positive cells and mast cells in frozen sections of multiple sclerosis brains. *J Neuroimmunol* 30: 169-77

56. Trapp BD, Peterson J, Ransohoff R, Rudick R, Mork S, Bo L (1998). Axonal transection in the lesions of multiple sclerosis. *N Engl J Med* 338: 278-285

57. Tsunoda I, Fujinami RS (1996). Two models for multiple sclerosis: experimental allergic encephalomyelitis and Theiler's murine encephalomyelitis virus. *J Neuropathol Exp Neurol* 55: 673-86.

58. Waxman SG (1998). Demyelinating diseases- new pathological insights, new therapeutic targets. *N Engl J Med* 338: 323-324.